Photochemistry of Benzylallene: Ring-Closing Reactions to Form Naphthalene

Joshua A. Sebree,[†,||] Nathanael M. Kidwell,[†] Talitha M. Selby,[‡] Brent K. Amberger,[§] Robert J. McMahon,[§] and Timothy S. Zwier*,[†]
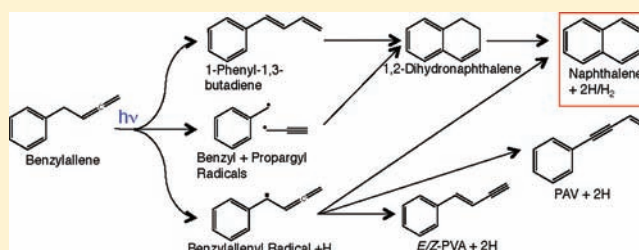
[†]Department of Chemistry, Purdue University, West Lafayette, Indiana 47907-2084, United States

[‡]Department of Chemistry, University of Wisconsin—Washington County, 400 University Drive, West Bend, Wisconsin 53095, United States

[§]Department of Chemistry, University of Wisconsin—Madison, Madison, Wisconsin 53706-1322, United States

Ⓢ *Supporting Information*

ABSTRACT: Conformer-specific, vibrationally resolved electronic spectroscopy of benzylallene (4-phenyl-1,2-butadiene) is presented along with a detailed analysis of the products formed via its ultraviolet photoexcitation. Benzylallene is the minor product of the recombination of benzyl and propargyl radicals. The mass-selective resonant two-photon ionization spectrum of benzylallene was recorded under jet-cooled conditions, with its S_0-S_1 origin at $37\,483$ cm^{-1}. UV−UV holeburning spectroscopy was used to show that only one conformer was present in the expansion. Rotational band contour analysis provided rotational constants and transition dipole moment direction consistent with a conformation in which the allene side chain is in the *anti* position, pointing away from the phenyl ring. The photochemistry of benzylallene was studied in a pump−probe geometry in which photoexcitation occurred by counter-propagating the expansion with a photoexcitation laser. The laser was timed to interact with the gas pulse in a short tube that extended the collisional region of the expansion. The products were cooled during expansion of the gas mixture into vacuum, before being interrogated using mass-selective resonant two-photon ionization. The UV−vis spectra of the photochemical products were compared to literature spectra for identification. Several wavelengths were chosen for photoexcitation, ranging from the S_0-S_1 origin transition (266.79 nm) to 193 nm. Comparison of the product spectral intensities as a function of photoexcitation wavelength provides information on the wavelength dependence of the product yields. Photoexcitation at 266.79 nm yielded five products (benzyl radical, benzylallenyl radical, 1-phenyl-1,3-butadiene, 1,2-dihydronaphthalene, and naphthalene), with naphthalene and benzylallenyl radicals dominant. At 193 nm, the benzylallenyl radical signal was greatly reduced in intensity, while three additional $C_{10}H_8$ isomeric products were observed. An extensive set of calculations of key stationary points on the ground state $C_{10}H_{10}$ and $C_{10}H_9$ potential energy surfaces were carried out at the DFT B3LYP/6-311G(d,p) level of theory. Mechanisms for formation of the observed products are proposed based on these potential energy surfaces, constrained by the results of cursory studies of the photochemistry of 1-phenyl-1,3-butadiene and 4-phenyl-1-butyne. A role for tunneling on the excited state surface in the formation of naphthalene is suggested by studies of partially deuterated benzylallene, which blocked naphthalene formation.

1. INTRODUCTION

In recent years, the chemical processes occurring in Titan's atmosphere have received considerable attention. With a makeup primarily of nitrogen and methane, it is thought to be similar in nature to the atmosphere of prebiotic Earth.[1] The Cassini satellite has returned an unprecedented quantity and quality of data probing the organic chemistry occurring in Titan's atmosphere. Recent flybys have revealed the presence of complex carbon and nitrogen containing molecules ranging in size up to several thousand daltons, thought to be a direct detection of polymeric "tholins", at much higher altitudes (~950 km) than previously imagined.[2,3] New photochemical models have made significant progress in describing the processes that lead from simple methane and nitrogen to the

organic haze particles that form Titan's aerosols.[4,5] However, because of a lack of experimental data, the products of many reactions leading to C_6 or higher products remain unknown and are simply listed as "polymer".[5] Several experimental studies have successfully demonstrated the formation of benzene and substituted benzenes in the gas phase by photoexcitation of small carbon chains.[6,7] With several pathways to the formation of single aromatic rings, attention is turning to mechanisms that lead to the formation of a second fused ring, which may be prototypical of pathways involved in the formation of larger fused ring systems.

As a photochemically driven atmosphere, neutral free radicals formed by photolysis are likely to play an important role in pathways that lead to naphthalene. Among the radicals of primary concern are resonance-stabilized radicals (RSRs), those in which the radical site is conjugated to a neighboring π-system. Due to the energetic stability accompanying delocalization of the radical site, further reaction is anticipated to be slow, and removal steps often are dominated by radical–radical recombination. The recombination of the propargyl radical (C_3H_3), one of the simplest RSRs, has been studied extensively for its possible role in the formation of benzene.[8,9]

In searching for facile pathways to naphthalene, one strategy is to follow a series of reactions involving RSR formation, subsequent recombination to form key stable intermediates, which then undergo photochemical excitation to form further RSRs or isomerize to produce naphthalene. In the case of naphthalene, one might anticipate that phenyl derivatives with saturated or unsaturated side chains are likely candidates as key intermediates. Should propargyl recombine with the benzyl radical, the smallest aromatic RSR, the two most stable products that could form are 4-phenyl-1-butyne and benzylallene (4-phenyl-1,2-butadiene), both $C_{10}H_{10}$ products.

benzyl radical   propargyl radical   4-phenyl-1-butyne   benzylallene
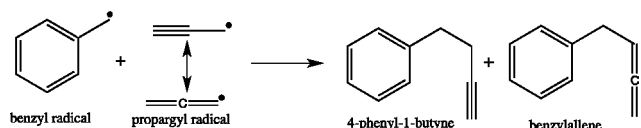
The flexibility inherent in the C_4 chain so formed allows for each product to possibly adopt two low-energy structural conformations, one with the chain pointed away from the benzene (*anti*) and the other with the side-chain over the benzene ring (*gauche*). The proximity of the π-systems in the *gauche* structure may play a role in ring-closure mechanisms. Thus, as a precursor to photochemical studies, the conformation specific spectroscopy of 4-phenyl-1-butyne[10] and several related C_{10} and C_{11} molecules[11−13] has been carried out under jet-cooled conditions. In the case of 4-phenylbutyne, it was found that both the *anti* and *gauche* conformers were present in the expansion. In this work, we will explore the spectroscopy of benzylallene and its subsequent photochemistry in some detail over a range of wavelengths from its S_0–S_1 origin (266.79 nm) to 193 nm. As we shall see, at all wavelengths in this range, benzylallene has naphthalene as one of its photochemical products.

Two RSRs were also detected as photoproducts, the benzyl radical and benzylallenyl radical. In a previous work, it was suggested that the benzylallenyl radical might play an important role in the formation of naphthalene.[14] In a recent paper from the Mebel group, a $C_{10}H_9$ potential energy surface was presented for the formation of naphthalene from the reaction of C_2H and styrene.[15] The benzylallenyl radical was included on this surface showing the possibility of a pathway to naphthalene. In the present study, this $C_{10}H_9$ surface is expanded to include the photolysis of benzylallene (to produce $C_{10}H_9$ + H) and its subsequent reactions. Along with the $C_{10}H_9$ surface, pathways on the $C_{10}H_{10}$ energy surface were also explored using ab initio calculations, providing a basis for postulating mechanisms for naphthalene formation. To better understand the mechanism by which naphthalene forms, preliminary photochemical studies of 4-phenyl-1-butyne and *trans*-1-phenyl-1,3-butadiene were also carried out with the results supporting a unimolecular rearrangement reaction

occurring on the $C_{10}H_{10}$ surface as the primary ring-closure pathway leading to naphthalene.

2. METHODS

Resonant two-photon ionization (R2PI), UV-holeburning (UVHB), and rotational band contours (RBC) of benzylallene were taken using a time-of-flight spectroscopy chamber that has been described previously.[6] Briefly, the sample was loaded in an external sample cell and entrained in argon (1 bar) at room temperature. The mixture was then expanded into a vacuum through a pulsed valve (RM Jordan) with an 800 μm orifice. Benzylallene was then detected using resonant two-photon ionization (R2PI) spectroscopy coupled with time-of-flight mass analysis. The tunable output of a doubled, Nd:YAG-pumped dye laser was used for the excitation and ionization steps. Rotational band contours (RBCs) were collected by scanning the laser over the origin transition at a higher resolution by angle tuning an intracavity etalon inserted into the oscillator cavity of the dye laser (0.08 cm^{-1} resolution in the UV).

Photochemical experiments were also carried out in the TOF chamber. A reaction channel (2 mm diameter × 7 mm long) was affixed to the valve face and is shown schematically in Figure 1.
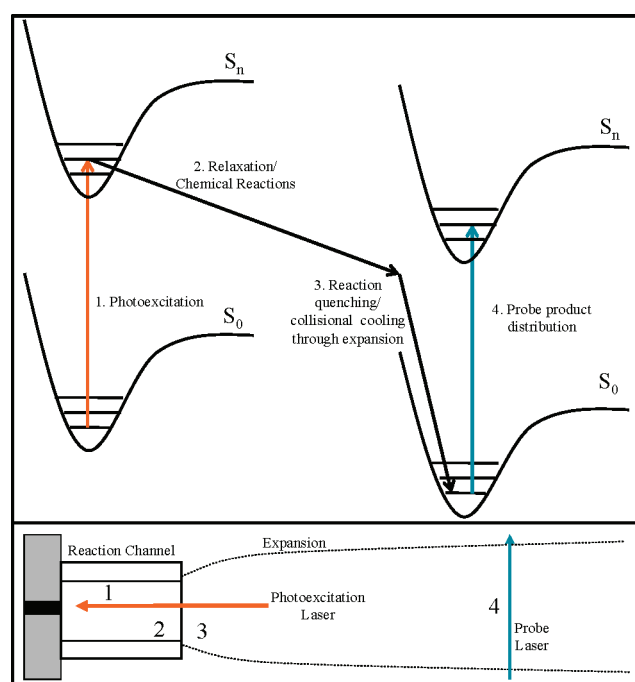
Figure 1. Energy level diagram (top) and schematic representation (bottom) of the photochemistry setup. Molecules are excited in the reaction channel (1) and allowed to relax and react (2). Upon exiting the channel (3) the reactions are quenched and products cooled before being probed in the ion source (4) region of a time-of-flight mass spectrometer. Scanning the probe laser provides R2PI spectra of the products at fixed excitation energy. Scanning the photoexcitation laser (action spectroscopy) while monitoring a given probe laser wavelength and product mass produces an action spectrum that maps the wavelengths at which that product is formed.

The photoexcitation laser, either the tunable UV from a doubled dye laser or 193 nm from a small ArF excimer laser, was directed up the reaction channel and timed to interact with the gas pulse inside the channel. Upon excitation, the molecule could undergo dissociation, isomerization, or bimolecular reaction. In the present study, no evidence for bimolecular reaction was observed. Upon leaving the channel, the final expansion quenches any reactions and cools the products down to their respective ground state zero-point vibrational levels. By adjusting the time delay between photoexcitation and probe
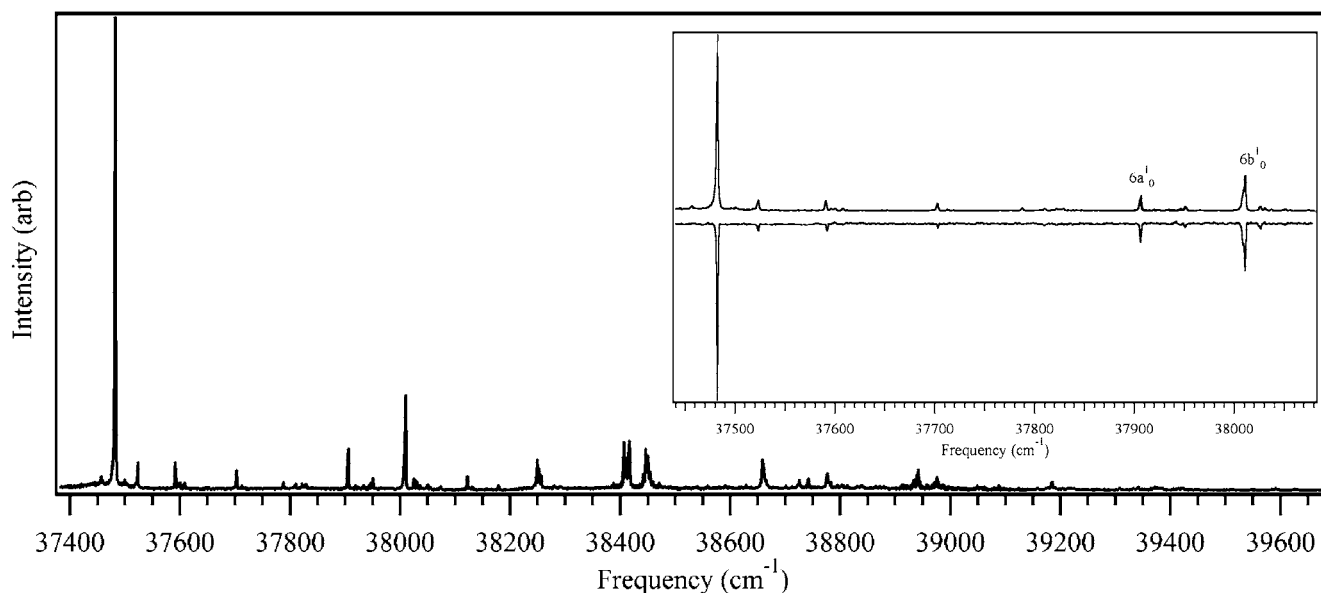
Figure 2. R2PI spectrum of benzylallene in the S_0-S_1 region. Inset: Comparison of the R2PI spectrum (top) with the UVHB (bottom) with a holeburn laser fixed on the band at 37 483 cm^{-1}. All transitions are present in the UVHB spectrum, proving that only one conformer was present in the expansion.

lasers, one can monitor products from photoexcitation at different positions along the reaction channel. Tracking the onset of a species as a function of the delay between the photoexcitation laser and the probe laser then is related to the sequence of product formation, if a multistep process is involved. The identity of the photoproducts could then be determined using R2PI and holeburning techniques.

To determine product ordering, two-dimensional timing diagrams were acquired for each product. To do this, the probe laser was fixed on a unique transition of the product of interest. The timings of the photoexcitation laser and pulsed-valve firing relative to the probe laser were then independently scanned, creating a two-dimensional plot. Depletion of a bezylallene reactant signal is used to map out the timing regions for excitation within the reaction tube. 90% contours of the products are used to inscribe timing regions where product peak intensities are within 10% of the peak maximum, providing a visual summary of the most probable arrival times of each product. Details of these diagrams and their interpretation are included in the Supporting Information.

As a means of testing whether products in the expansion were formed by gas-phase excitation of benzylallene, action spectroscopy was employed. To record an action spectrum, the photoexcitation laser is scanned through the vibronic transitions of the S_0-S_1 spectrum of benzylallene, while the probe laser is fixed on a transition due to a particular product in its R2PI spectrum. By employing a timing set for photochemical product detection, a product signal should only be detected when the photoexcitation laser is resonant with a vibronic transition of benzylallene.

Samples of 4-phenyl-1-butyne and *trans*-1-phenyl-1,3-butadiene were purchased from Sigma-Aldrich and used without further purification. Benzylallene and deuteriated isotopomers were synthesized by procedures described in the Supporting Information. Prior to use, the benzylallene in hexane was added to cotton, and the hexanes were allowed to evaporate from the sample. The cotton with the benzylallene was then loaded in to the pulsed valve for use.

Key stationary points on the ground state $C_{10}H_{10}$ and $C_{10}H_9$ potential energy surfaces were mapped out to explore possible reaction pathways from benzylallene to the observed products. Starting structures of reactants, products, proposed intermediates, and transition states connecting them were optimized using density functional theory (DFT) with a Becke3LYP[16,17] functional and 6-311G(d,p) basis set. Harmonic vibrational frequencies were computed at the same level of theory to obtain zero point energies

(ZPEs) for each species. These calculations were performed using Gaussian 09.[18] Rotational band contour simulations were carried out using JB95 software.[19]

3. RESULTS AND ANALYSIS

3.1. Benzylallene Spectroscopy. Figure 2 presents the R2PI spectrum of benzylallene in the S_0-S_1 region. The spectrum is strikingly similar to those of similar alkylbenzenes.[10,11,13,20] Because of the possible presence of two conformers in the expansion, UV−UV holeburning was performed sitting on the strong transition at 37 483 cm^{-1}. It was found that all the observed transitions belong to a single conformer (Figure 2 inset). The most intense band has been assigned as the S_0-S_1 origin and is less than 150 cm^{-1} to the red of the two conformers of 4-phenylbutyne (37 617 and 37 620 cm^{-1} for the *gauche* and *anti* conformers, respectively).[10] In addition, the features labeled $6a^1_0$ and $6b^1_0$ are characteristic ring deformation modes (Varsanyi notation[21]) for molecules of this nature.

Because of the interest in this molecule as a photochemical precursor to bicyclic rings, it was important to identify the preferred conformation taken up by the side chain. Figure 3a shows the optimized structures (B3LYP/6-311G(d,p)) for the *gauche* and *anti* conformers of benzylallene. According to the calculations, the *anti* conformer is more stable by 0.8 kcal/mol. The rotational band contour of the S_0-S_1 origin transition of benzylallene was taken at a higher resolution of 0.08 cm^{-1}. Because of the sensitivity of the transition dipole moment (TDM) to the position of the side chain[22,23] in phenyl derivatives, past studies have used the shape of the rotational band contour to assign conformations based on the comparison with the predictions of calculations, using the rotational constants from HF and CIS calculations and the TDM direction from the CIS results.[10,24] The result, calculated using JB95,[19] is shown in Figure 3b. The calculations predict the *gauche* conformer to possess a pure C-type band contour, while the *anti* conformer should have a hybrid rotational band contour with TDM $\mu_a^2:\mu_b^2:\mu_c^2 = 69:27:4$. While the predicted
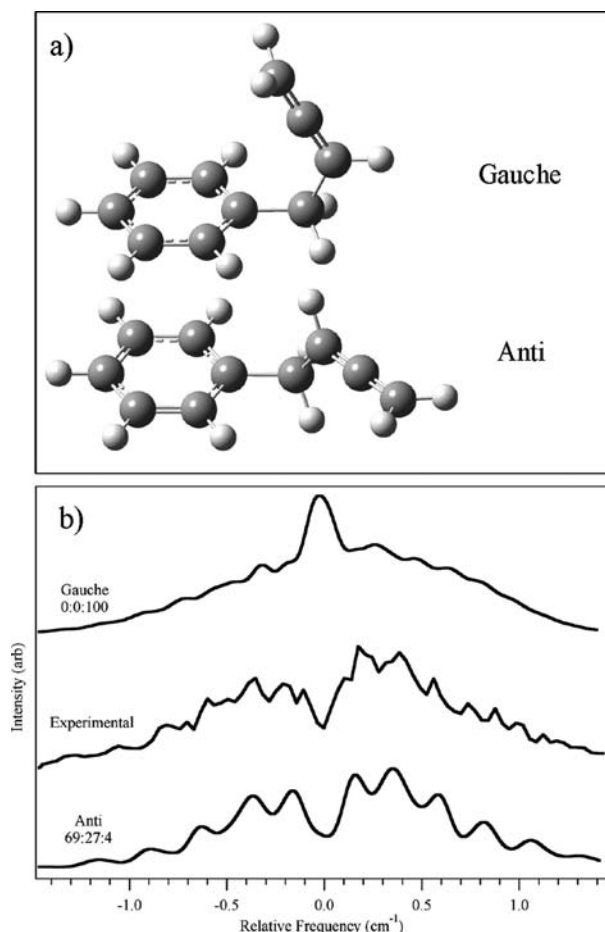
Figure 3. (a) Calculated structures of *gauche* and *anti* conformers of benzylallene. (b) Experimental rotational band contour of benzylallene (middle trace) compared to simulated contours[19] for *gauche* (top) and *anti* (bottom) using rotational constants and TDM direction from CIS calculations.

band contour for the *gauche* conformer is a poor match with experiment, the hybrid rotational band contour predicted by the calculations for the *anti* conformer very closely matches the experimental band contour. As a result, the observed conformer is assigned as *anti*-benzylallene. This contour is also similar in shape to those of *anti*-4-phenyl-1-butyne[10] and *anti*-4-phenyl-1-butene,[13] further strengthening the assignment.

3.2. Photochemistry. The photochemistry of benzylallene was initially explored using 193 nm as the photoexcitation wavelength. The laser was aligned to counter-propagate the expansion, and timing was set such that the gas pulse and the laser would intersect within the reaction channel. A mass spectrum was collected using 266 nm light as the ionization laser. The difference mass spectrum in Figure 4 was collected by subtracting a mass spectrum with the photochemistry laser absent from one with it present. The peaks in the resulting mass spectrum correspond to those products with an appreciable absorption cross-section at 266 nm. To identify the various products in each mass channel, the probe laser was scanned while monitoring the intensity of each mass channel.

Figure 5 shows the one-color R2PI scans for the closed-shell species with m/z = 128 and 130 amu (Figure 5a and 5b, respectively), corresponding to $C_{10}H_8$ (+2H, H_2) photodissociation and $C_{10}H_{10}$ isomeric products, respectively. By comparing the observed spectra to the known spectra of
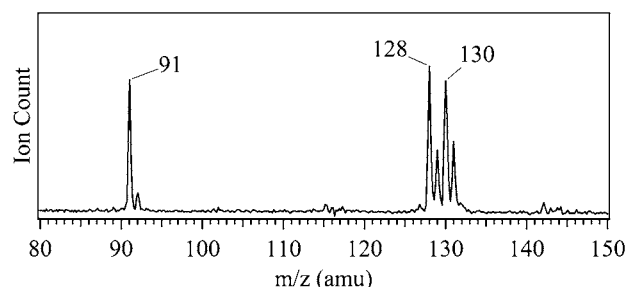

Figure 4. Benzylallene product difference mass spectrum using 193 nm light as the photoexcitation laser and 266 nm light for ionization.

possible isomers from the literature, it is possible to clearly identify four $C_{10}H_8$ photochemical products: *E*- and *Z*-phenylvinylacetylene (PVA),[25,26] 1-phenyl-but-3-en-1-yne (PAV),[13,27] and naphthalene.[28] The absorptions responsible for these identifications are labeled in the figure.
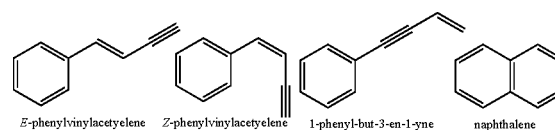

In the m/z = 130 channel (Figure 5b), the ion gain signals were identified as 1-phenyl-1,3-butadiene[29] and 1,2-dihydronaphthalene.[13,30] The depletions on the blue edge of the spectrum ($\sim$37 500 cm^{-1}) correspond to the loss of benzylallene reactant. To our knowledge, the identification of naphthalene and 1,2-dihydronaphthalene as products constitutes the first evidence of a gas-phase-substituted benzene
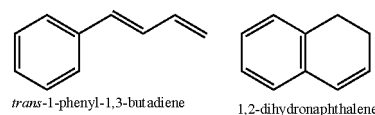
undergoing a ring-closing mechanism following UV photoexcitation.

Two open-shell resonance stabilized radicals (RSRs) were also identified as photochemical products, with 2C-R2PI spectra shown in Figure 6. These are identified as a benzyl radical (m/z = 91)[6] and a benzylallenyl radical (m/z =129).[14] It is assumed that the propargyl radical is also present as a product in equal proportion to the benzyl radical, although it was not directly detected in this study.
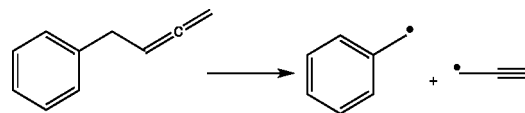

In an effort to better understand the time dependence of product formation, timing scans were taken of each product, and the resulting diagonal cut through the 2D plot was extracted as an approximate time profile for formation of each product.

We use these scans to determine the order of product formation. As shown in Figure 7, 90% contours from each timing diagram lie along the diagonal determined from the 193 nm depletion scan (Figure S1, Supporting Information). These contours are overlaid on the reactant depletion scan.

On the basis of this analysis, 1-phenyl-1,3-butadiene and 1,2-dihydronaphthalene are found to be produced earliest in time.
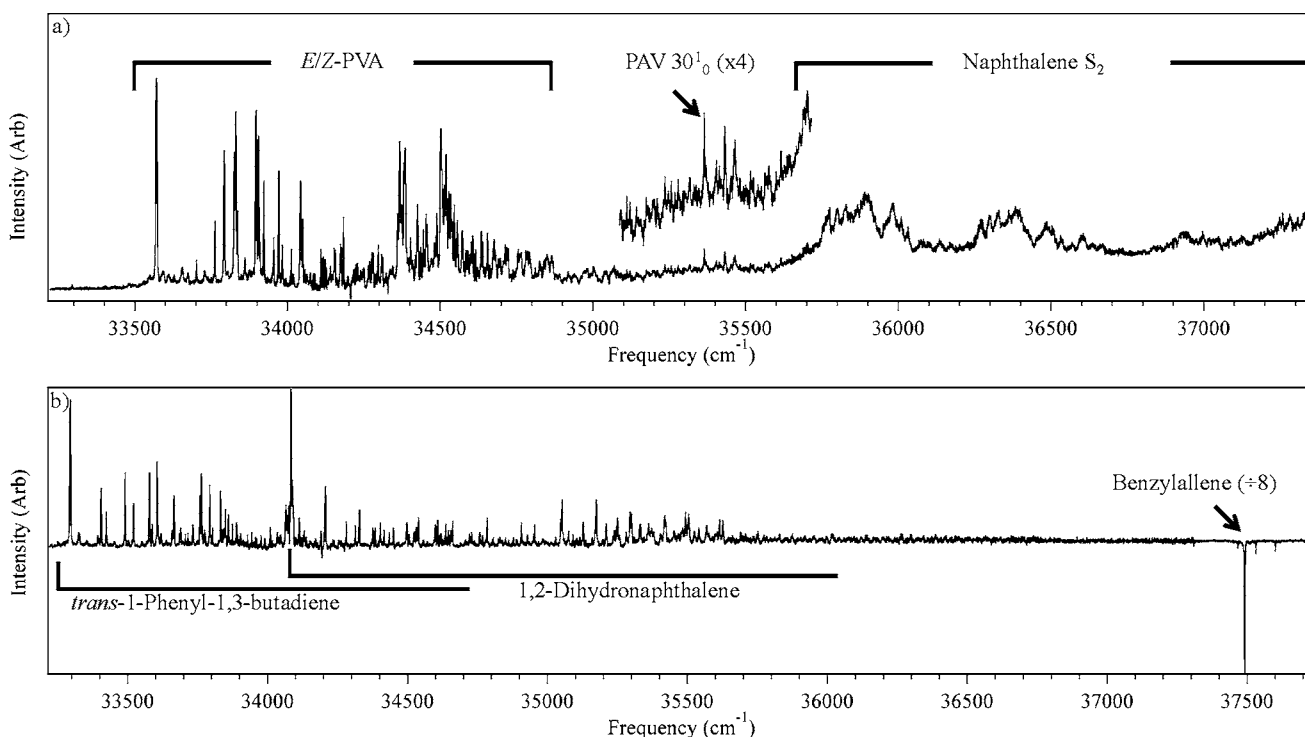
Figure 5. (a) R2PI spectra of the m/z 128 photoproducts formed following 193 nm excitation. Products are identified as PVA, PAV, and naphthalene. (b) R2PI spectra collected in the m/z 130 mass channels showing gains corresponding to the formation of *trans*-1-phenyl-1,3-butadiene and 1,2-dihydronaphthalene products and depletions corresponding to the loss of benzylallene reactant.
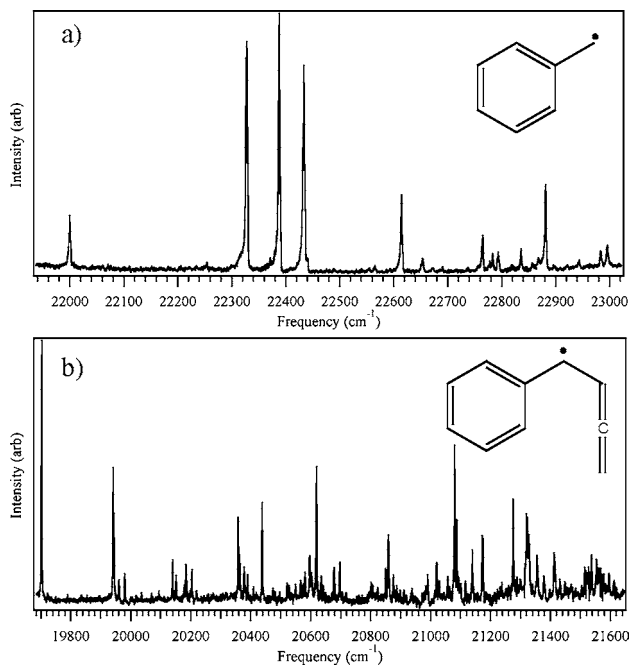

Figure 6. 2C-R2PI spectra collected in the (a) m/z 91 and (b) m/z 129 mass channels corresponding to benzyl and benzylallenyl radicals, respectively.

These are followed by *E*- and *Z*-PVA, PAV, and naphthalene, with naphthalene peaking about 15 μs later in time than the earliest time profile product (Figure 7b). Benzyl and benzylallenyl radicals (not shown) had timing profiles with turn-on times similar to 1-phenyl-1,3-butadiene and 1,2-dihydronaphthalene. The large number of products observed from 193 nm excitation is in keeping with the large internal energy associated with absorption at this wavelength (~6.43 eV), which is sufficient for a number of isomerization and dissociation steps to occur in competition with the collisional cooling that accompanies expansion from the reaction channel. A detailed discussion of possible mechanisms is deferred until after the potential energy surfaces are presented.

To gain more insight into the processes that lead to naphthalene, the photoexcitation laser was switched to 266.79 nm, the wavelength of the $S_0–S_1$ origin of benzylallene. At 4.65 eV, this is the lowest-energy photon that benzylallene can absorb efficiently via electronic transitions. As expected, there were significant differences in the observed product distributions from those at 193 nm. Table 1 summarizes the relative product distributions at 266.79 and 193 nm photoexcitation wavelengths. Product detection via R2PI methods is a powerful tool for the unequivocal determination of the structural isomers present. However, determination of absolute product yields requires knowledge of R2PI efficiencies of each product at the chosen wavelength for their detection. These data are not currently available for the products of interest. Furthermore, the two radicals, benzyl and benzylallenyl, were detected in 2C-R2PI with 220 nm as the second photon. As a result, we report the relative ion signal of each product based on their intensity with the probe laser fixed on their respective $S_0–S_1$ origins (or a strong vibronic feature), normalized with respect to the signal present when monitoring the 35 900 cm^{-1} band of naphthalene from 193 nm excitation using 1 mJ/pulse laser power for photoexcitation.

Of the eight observed products from 193 nm irradiation, only five were observed at 266.79 nm. The three products not observed at this lower excitation energy are the three non-naphthalene $C_{10}H_8$ isomers, *E/Z*-PVA and PAV, suggesting an energy barrier for their formation between 4.65 and 6.43 eV.
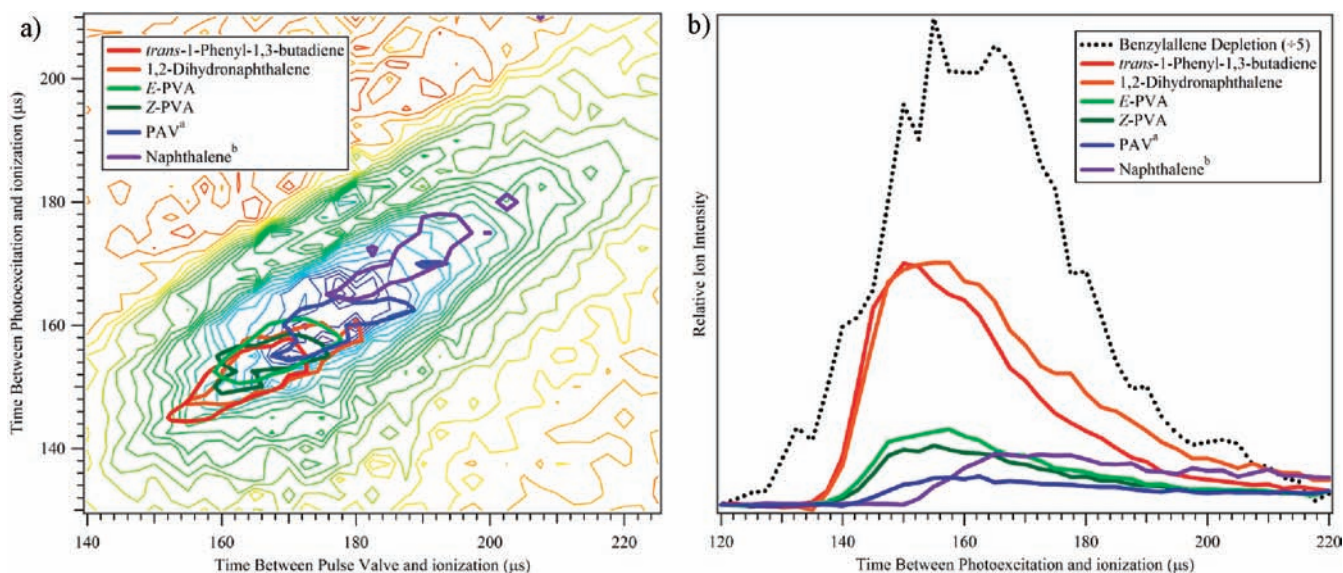
Figure 7. (a) 90% contours from product timing scans overlaid on the 193 nm benzylallene depletion scan. (b) Diagonal slices through the reaction plateau of each timing diagram show the ordering of products. Benzylallenyl and benzyl radicals (not shown) show profiles peaking at times similar to 1-phenyl-1,3-butadiene, indicating they are also primary products. [a]PAV scans were carried out by monitoring its 30^1_0 vibronic band.[27] [b]Naphthalene scans were recorded using the S_2 vibronic peak at ~35 900 cm^{-1}.

Table 1. Relative[a] Origin Intensities of Photoproducts at Various Excitation Energies

				intensities at excitation wavelength (nm)					
m/z	product	origin (cm^{-1})	266.79	250	240	230	220	193	ref
91	benzyl radical	22000	0.3	0.01	0.1	0.3	1.4	1.5	6
128	E-PVA	33578	--	--	--	--	--	1.8	25, 26
128	Z-PVA	33838	--	--	--	--	--	1.5	25, 26
128	PAV	35388[b]	--	--	--	--	--	0.2[b]	13, 27
128	naphthalene[c]	~35900[c]	3.0	0.01	0.01	0.01	0.01	1.0	28
129	benzylallenyl radical	19703	27	1.6	3.9	4.1	0.6	0.3	14
130	1-phenyl-1,3-butadiene	33315	0.3	<0.01	<0.01	<0.01	<0.01	4.2	29
130	1,2-dihydronaphthalene	34086	0.3	<0.01	<0.01	<0.01	<0.01	3.9	13, 30

[a]Intensities normalized to the naphthalene vibronic band at ~35 900 cm^{-1} from 193 nm excitation. [b]30^1_0 vibronic band. [c]Naphthalene S_2 vibronic band.

Of the five products detected, 1-phenyl-1,3-butadiene and 1,2-dihydronaphthalene were ~10 times smaller at 266.79 nm, with a similar five-fold decrease seen in the benzyl radical. The benzylallenyl radical, however, was almost 100-fold larger in size. Quite unexpectedly, there was also a 3-fold increase in the amount of observed naphthalene (Figure 8). Our expectation is that the absorption cross section of benzylallene is likely to be substantially greater at 193 nm than at 266.74 nm. If so, the increase in product yield at longer wavelength is a clear
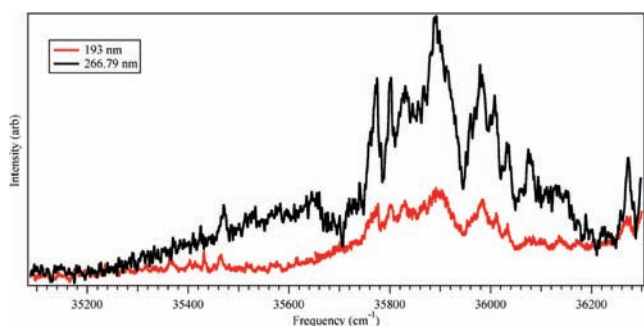

Figure 8. Comparison of the S_0–S_2 region of naphthalene collected using 193 nm (black) and 266.79 nm (red) photoexcitation wavelengths. In both cases, 1 mJ/pulse photoexcitation laser power was used.

indication that the absolute product yield of naphthalene is greater at the S_0–S_1 origin than at 193 nm.

To prove that naphthalene was forming exclusively from the photoexcitation of benzylallene, an action spectrum was recorded by monitoring a characteristic naphthalene product absorption (35 900 cm^{-1}) while tuning the photoexcitation laser through the S_0–S_1 origin region of benzylallene. As shown in Figure 9, the naphthalene product signal follows the excitation profile of benzylallene in every detail. The difference in width between the jet-cooled spectrum of benzylallene (top) and the action spectrum reflects the intermediate temperature in the reaction channel which was shown previously to be ~75 K.[7] The other products formed from 266.79 nm photoexcitation had action spectra similar to that in Figure 9.

Wavelength-dependent signals for each product at 250, 240, 230, and 220 nm were also recorded and are included in Table 1. Laser powers of ~1 mJ/pulse were used at each excitation energy. The relative product signal sizes for naphthalene, 1-phenyl-1,3-butadiene, and 1,2-dihydronaphthalene remained similar throughout the range. PAV and E- and Z-PVA were only detected at 193 nm. If energetic constraints are responsible for their lack of detection, this places a lower limit on the barriers to their formation of 5.64 eV (220 nm).
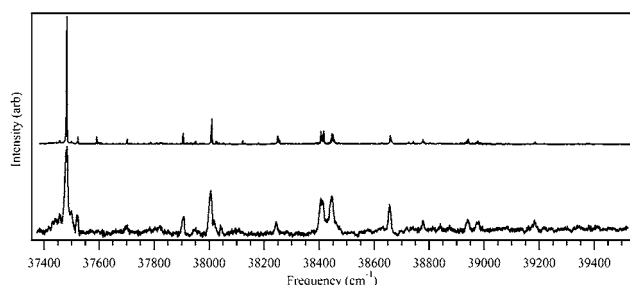
Figure 9. Comparison between the R2PI spectrum of benzylallene (top trace) and the action spectrum monitoring the naphthalene photochemical product (bottom trace). The action spectrum was recorded by recording the naphthalene product R2PI signal (with detection wavelength fixed at $35\,900$ cm^{-1}) while scanning the photoexcitation laser over vibronic transitions due to benzylallene. Results were similar for the other compounds observed using 266.79 nm light.

The most dramatic wavelength-dependent shift in product distribution occurs between 230 and 220 nm, where the benzyl radical product increases markedly in intensity, seemingly at the expense of the benzylallenyl radical signal. It is postulated that the observed changes correspond to accessing a higher excited state of benzylallene that favors dissociation to the benzyl radical, while the S_1 state favors dissociation to the benzylallenyl radical. As will be discussed in more detail below, the dissociation pathway for benzyl + propargyl formation is below that of the benzylallenyl radical (+H), indicating that the shift in product distribution is more likely the result of wavelength-dependent or competitive pathways. Finally, with the increase of naphthalene and the presence of other products at 193 nm, it is postulated that several pathways become accessible at energies between 5.64 and 6.43 eV.

4. DISCUSSION

4.1. Potential Energy Surfaces. To better understand the processes by which naphthalene and the other products are formed, key stationary points on the potential energy surfaces for $C_{10}H_{10}$ and $C_{10}H_9$ product pathways were calculated using DFT (B3LYP 6-311G(d,p)) methods. In what follows,

we divide discussion along three main pathways to forming products: (i) unimolecular rearrangement ($C_{10}H_{10}$ unimolecular surface) followed by the loss of two hydrogens either as 2H or H_2, (ii) dissociation to and subsequent recombination of benzyl and propargyl radicals ($C_{10}H_{10}$ bimolecular surface) followed by the loss of two hydrogens either as 2H or H_2, or (iii) H-atom loss to a benzylallenyl radical with subsequent rearrangement ($C_{10}H_9$ surface) and possible further H-atom loss to $C_{10}H_8$ products.

Attention is focused throughout this discussion on ground-state pathways accessed following internal conversion, to see whether the observed products can be accounted for in this way. The possibility that excited state surfaces might also be involved must be recognized at the outset. In particular, the experimental arrangement used here, in which photoexcitation is followed by a collisional cooling step prior to spectroscopic interrogation, prevents any direct interrogation of excited state processes that might be occurring. Transient absorption or time-resolved photoelectron spectra of benzylallene under collision-free conditions are needed to address these issues further. Theoretical work aimed at mapping out these surfaces and the crossings/conical intersections between them will also be required.

On the ground state surface, formation of naphthalene (+2H, H_2) following unimolecular isomerization on the $C_{10}H_{10}$ surface (Figure 10) first requires a 1,3-hydrogen shift from benzylallene to form 1-phenyl-1,3-butadiene, occurring over a 60.0 kcal/mol barrier. Ring closure of 1-phenyl-1,3-butadiene, followed by a 1,5-hydrogen shift assisted by aromatization,[31] results in 1,2-dihydronaphthalene. Naphthalene is then formed by loss of two hydrogens, either individually or as H_2 if the first hydrogen facilitates the loss of the second. The reaction time profiles showing the order of 1-phenyl-1,3-butadiene, 1,2-dihydronaphthalene, and naphthalene are consistent with this $C_{10}H_{10}$ pathway, where benzylallene must first go through 1-phenyl-1,3-butadiene prior to ring closure and hydrogen loss. With a calculated rate-limiting barrier of 76.0 kcal/mol (for naphthalene +2H formation), the energy provided by 266.79 nm light (107.2 kcal/mol) is clearly sufficient to form naphthalene via this pathway.
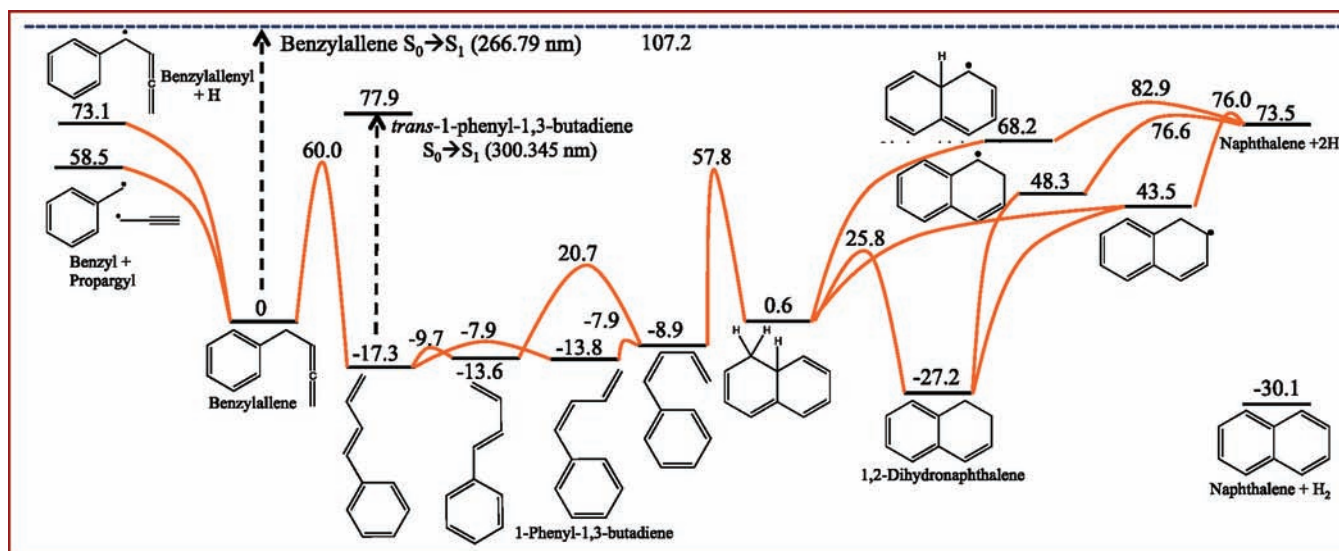
Figure 10. $C_{10}H_{10}$ unimolecular potential energy surface calculated using the B3LYP/6-311G(d,p) level of theory. All values are ZPE corrected with units of kcal/mol.
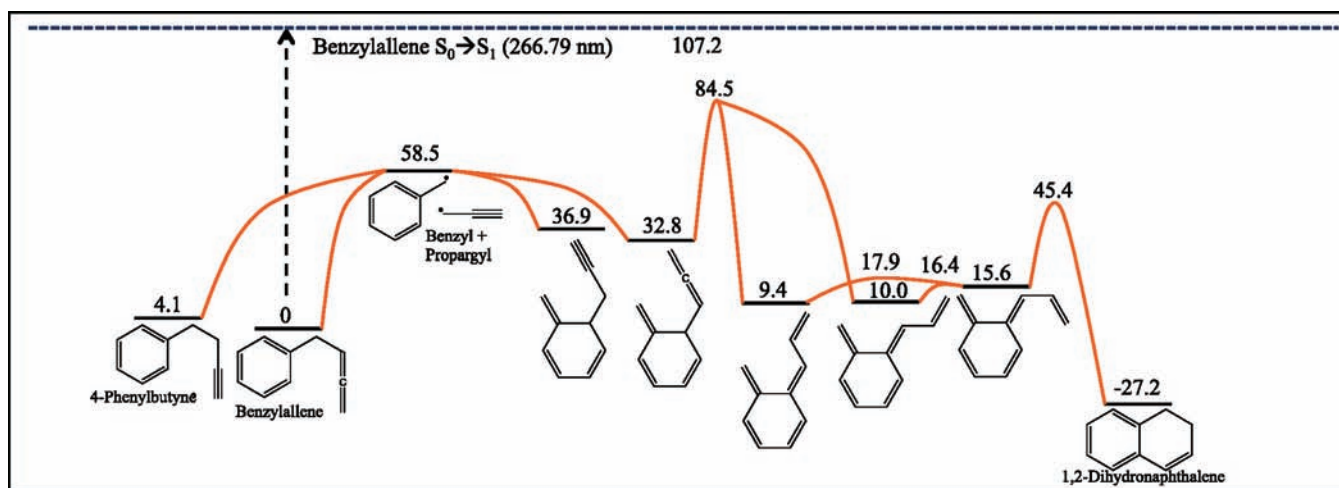
Figure 11. Portion of the $C_{10}H_{10}$ potential energy surface accessed by recombination of benzyl + propargyl radicals, calculated at the DFT B3LYP/6-311G(d,p) level of theory. Because of the lack of experimental evidence in support of this pathway, only the simplest relevant pathway is shown. Pathways leading from 1,2-dihydronaphthalene to naphthalene are the same as those in Figure 10. All values are ZPE corrected with relative energies given in kcal/mol.

It is also important to note that of the two dissociation pathways (benzylallenyl radical plus H and benzyl plus propargyl radicals) the benzyl plus propargyl pathway is favored by 14.6 kcal/mol and is of similar energy to the first step in the isomerization pathway (60.0 kcal/mol). These dissociation pathways are thus in direct competition to intramolecular isomerization pathways.

Because photoexcitation occurs as the gas mixture traverses the reaction tube, it is important to consider recombination pathways as this is not a collision-free environment. In particular, with the detection of the benzyl radical as a primary product, it is also important to consider bimolecular pathways that involve the recombination of benzyl and propargyl radicals. Pathways unique to this scenario are shown in Figure 11.

In this scenario, the initial step following photoexcitation is photodissociation of benzylallene to benzyl + propargyl radicals, which could subsequently recombine in several ways. The benzyl radical has three energetically favorable bonding sites: the original CH_2 site, ortho to the CH_2 group on the ring, or para to the CH_2. The meta position of the benzyl radical has little radical character, making it unfavorable as a position of attack for the propargyl radical since it would create a highly unstable diradical. In addition, the propargyl radical can recombine at either its $-CH$ terminus or its $-CH_2$ terminus. Each recombination can then have several local minima with the propargyl/allene moiety having different orientations with respect to the benzene ring, giving a total of 14 isomeric structures, with relative energies provided in Table 2. Of the immediate recombination products, benzylallene and 4-phenyl-1-butyne are the lowest in energy, while the ortho-substituted adducts needed to make naphthalene are the highest.

With 4-phenyl-1-butyne formation being favored by more than 25 kcal/mol over any of the ortho-substituted compounds, one would expect that 4-phenyl-1-butyne would be a significant product if recombination of benzyl and propargyl radicals was occurring under the present experimental conditions. Careful searches for 4-phenyl-1-butyne transitions in R2PI produced no measurable signal, providing strong evidence that this pathway is not facile on the time scale and under the conditions of our experiment. In addition, to form naphthalene from the ortho-allene recombination product, a 1,3-hydrogen shift with a

Table 2. Structures and Relative Energies (kcal/mol) of the Possible Benzyl Plus Propargyl Recombination Products[b]

Structure	Recombination motif	Relative Energies[a]
	Benzylallene	0.0, 0.8
	4-Phenyl-1-butyne	4.1, 4.9
	ortho-allene	32.8, 34.0, 34.3
	ortho-propyne	36.9, 37.6, 38.6
	para-allene	29.0, 30.3
	para-propyne	33.4, 34.6

[a]Multiple values listed correspond to conformational isomers. [b]Energy values are ZPE corrected, at the DFT B3LYP/6-311G(d,p) level of theory.

relative barrier of 84.5 kcal/mol must first be overcome, followed by rearrangement to 1,2-dihydronaphthalene as a necessary intermediate. While this barrier is still below that of the excitation photon, bimolecular reactions are generally anticipated to be formed preferentially at longer reaction times, which disagrees with the early experimental onset of 1,2-dihydronaphthalene as a product (Figure 7).

With the large amount of benzylallenyl radical detected, it is important to consider reactions occurring on the $C_{10}H_9$ potential energy surface after formation of the benzylallenyl radical. Figure 12 presents the calculated $C_{10}H_9$ surface leading to formation of several of the observed $C_{10}H_8$ products

1160

dx.doi.org/10.1021/ja209189g | *J. Am. Chem. Soc.* 2012, 134, 1153−1163
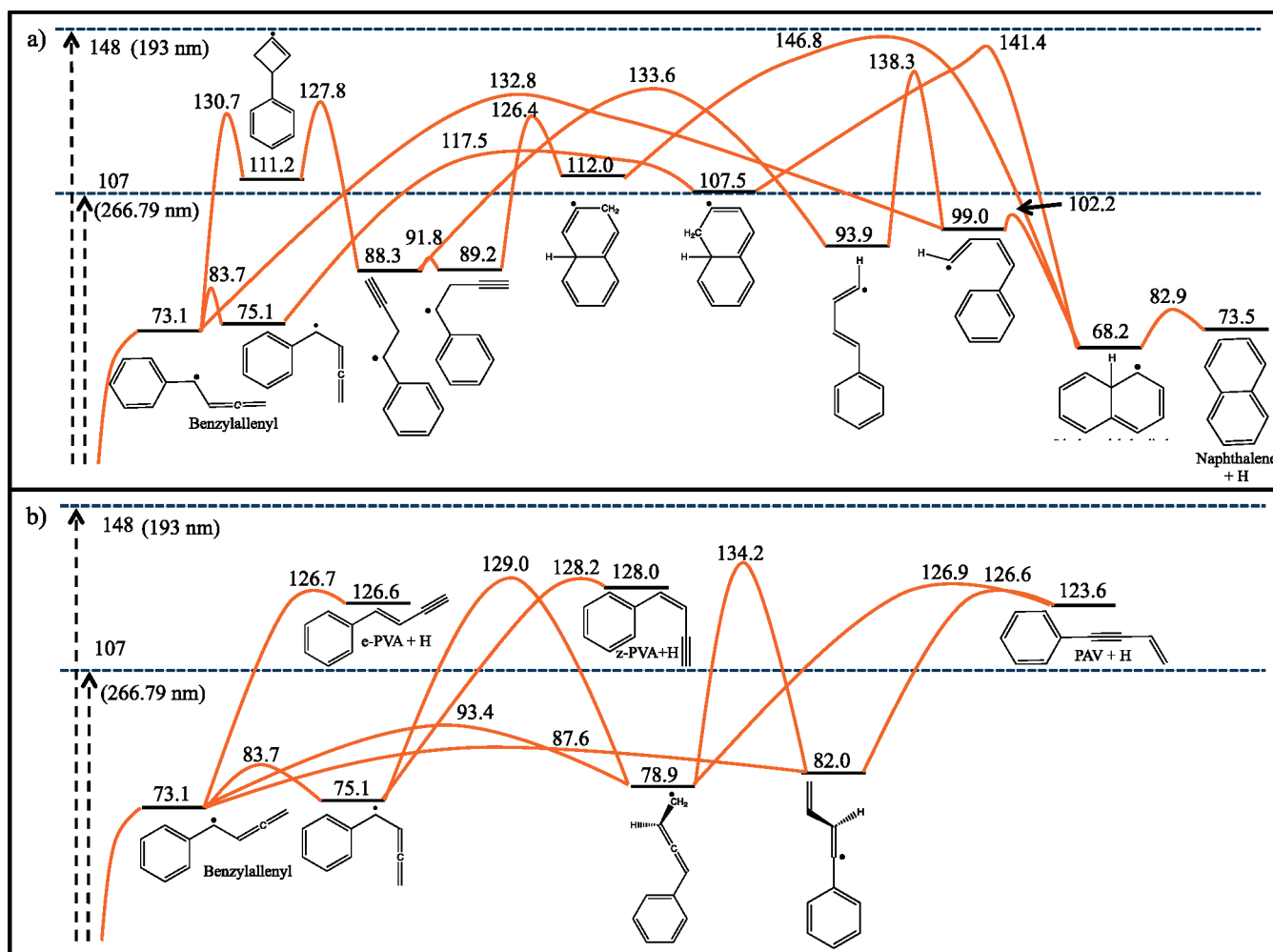
Figure 12. $C_{10}H_9$ potential energy surface showing (a) the formation of naphthalene and (b) PVA and PAV, from the benzylallenyl radical, calculated at the DFT B3LYP/6-311G(d,p) level of theory. All values are ZPE corrected with units of kcal/mol. Parts of this surface have been adapted from ref 15, with numerical values from the DFT calculations. See Supporting Information for comparison to G3(CC,MP2).

following H-atom loss, calculated at the DFT B3LYP/6-311G(d,p) level of theory. Parts of the surface have been adapted from a recent paper by Landera et al. carried out using a G3(CC,MP2) method.[15] For consistency, all energies in the table are from the DFT calculations; however, a side-by-side comparison (Table S1, Supporting Information) shows the DFT calculations to be generally close (average error ∼5 kcal/mol), with DFT overestimating the barriers. The most striking feature of this surface is that to form any of the observed products the reaction must overcome barriers in excess of 107.2 kcal/mol. As a result, at 266.79 nm, this surface cannot be used to explain the formation of naphthalene or any of the other observed products. This may explain the large amount of benzylallenyl radical observed at this wavelength. With 193 nm light, the $C_{10}H_9$ surface nicely shows how PVA and PAV can form via the rearrangement and/or loss of one hydrogen from the benzylallenyl radical (Figure 12b). At the same time, the opening of these channels also accounts for the small amount of the benzylallenyl radical observed at higher excitation energies.

As a final note, photoexcitation of benzylallene at 220 nm (130.0 kcal/mol) is very near the top of the limiting barriers for PAV or PVA formation. This is in agreement with the observation that no PAV or PVA was observed using 220 nm

light since small discrepancies between the real and calculated barriers may block or minimize their formation.

4.2. Pathways to Naphthalene. To gain more insight as to which mechanisms may be important in the formation of naphthalene, preliminary photochemical studies were carried out on several $C_{10}H_{10}$ isomers, focusing on the issue of whether their photoexcitation can form naphthalene.

With the prediction of 1-phenyl-1,3-butadiene as a key intermediate between benzylallene and naphthalene, photochemical studies were conducted on 1-phenyl-1,3-butadiene, with the photochemistry laser fixed on its $S_0–S_1$ origin (300.345 nm), while the probe laser was scanned over the naphthalene $S_0–S_2$ region. The initial photoexcitation energy for this experiment is included in Figure 10. The results (Figure 13a, black trace) showed that naphthalene was readily formed at the S_1 origin of trans-1-phenyl-1,3-butadiene. Furthermore, action spectroscopy confirmed that the naphthalene product was formed following photoexcitation of gas-phase 1-phenyl-1,3-butadiene (Figure 13b).

We have not carried out a full search for other products observed in 1-phenyl-1,3-butadiene photochemistry, nor have we probed other photoexcitation wavelengths. These are tasks left for future work. The detection of naphthalene from 1-phenyl-1,3-butadiene is not only consistent with the unimolecular pathway
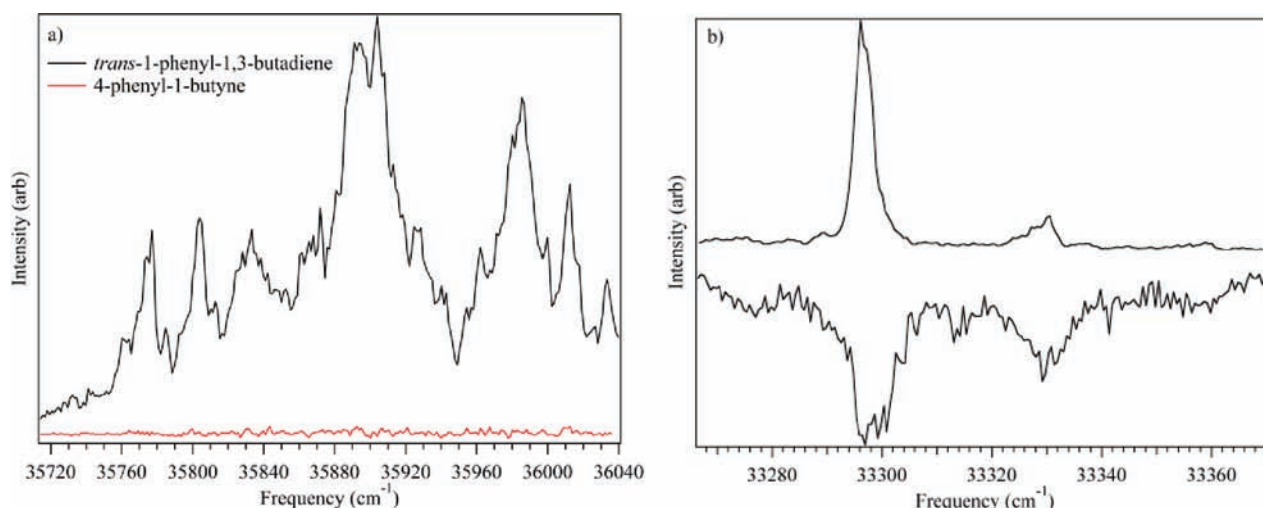
Figure 13. (a) R2PI scan over the S_0-S_2 vibronic bands of naphthalene products formed from photoexcitation of *trans*-1-phenyl-1,3-butadiene (black) and 4-phenyl-1-butyne (red) at their respective S_0-S_1 origins. Note the lack of signal from 4-phenyl-1-butyne. (b) Action spectrum of the S_0-S_1 origin region of *trans*-1-phenyl-1,3-butadiene (bottom) while detecting naphthalene, compared to the R2PI spectrum of *trans*-1-phenyl-1,3-butadiene (top).

proposed in Figure 10 but also sets a limit of 77.9 kcal/mol as the maximum barrier for naphthalene formation relative to benzylallene (95.2 kcal/mol compared to *trans*-1-phenyl-1,3-butadiene). The facile interconversion of 1-phenyl-1,3-butadiene to naphthalene was also observed in pyrolysis studies of 1-phenyl-1,3-butadiene carried out at 700 °C.[32]

A preliminary study of the photochemistry of 4-phenyl-1-butyne was also performed. While this species is not among the observed photoproducts from benzylallene, it is the primary product anticipated for recombination of benzyl and propargyl radicals. Given the similar energies of 4-phenyl-1-butyne and benzylallene and the similar S_0-S_1 origins of 37 617 and 37 620 cm^{-1} for the two isomers, the initial internal energy associated with photoexcitation of 4-phenyl-1-butyne is only slightly shifted from that in benzylallene. Photoexcitation at the S_0-S_1 origin resulted in a benzyl radical signal similar in size to that produced from benzylallene excitation. However, despite careful searches for its presence, naphthalene was not observed (Figure 13, red trace). This argues against benzyl plus propargyl recombination as a facile pathway to naphthalene under our experimental conditions and instead supports the notion of a unimolecular process following excitation of benzylallene, leading to ring closure and then on to naphthalene following H-atom/H_2 loss. It is important to note that if the benzyl and propargyl radicals were to thermalize prior to recombination to form benzylallene there would not be enough energy to overcome the subsequent barriers to naphthalene formation. In comparison, the unimolecular reaction of benzylallene to form 1-phenyl-1,3-butadiene proceeds via a unique 1,3-H-atom shift. Any similar shift in 4-phenyl-1-butyne would result in the formation of unstable diradical species.

In a final attempt to elucidate more about the mechanism of naphthalene formation, a sample of partially deuterated benzylallene was synthesized (see Supporting Information for full description and R2PI spectra) for study. The synthesized sample was determined to contain both α,α-dideuteriobenzylallene and α,α,β-trideuteriobenzylallene. R2PI scans showed that the S_0-S_1 origins of the -d_2 and -d_3 species were shifted by 13 and 48 cm^{-1} to the blue of benzylallene-h_8. This shift allowed for the selective excitation of each species individually

simply by choice of photoexcitation laser wavelength. However, no deuteriated naphthalenes were observed to come from either the -d_2 or -d_3 species upon excitation. As a confirmation that experimental conditions had not changed, a small amount of benzylallene-h_8 was added to the deuteriated sample. Scanning the excitation laser over the origins of the three isotopologues resulted in the detection of naphthalene-h_8 only when benzylallene-h_8 was excited, while no deuteriated naphthalenes were detected when -d_2 and -d_3 precursors were excited. Because the barriers in Figure 10 are not expected to change significantly upon deuteriation, this may be an indication that tunneling is playing a role in the 1,3-hydrogen shift in going from benzylallene to 1-phenyl-1,3-butadiene. On the ground state surface (Figure 10), tunneling is unlikely to play a role given the excitation energy (107 kcal/mol) relative to the barrier height (60 kcal/mol). However, the initial steps of the reaction may be occurring in the excited state, where barriers to reaction are still not known. The dynamics of this barrier crossing may be very sensitive to mass effects, preventing the shift when deuterium is involved. To better follow the effects of deuteriation and, in turn, how naphthalene is formed, pure samples of selectively deuteriated benzylallene and 1-phenyl-1,3-butadiene should be studied under similar conditions looking for naphthalene formation. This would help shed light on the excited versus ground state nature of the first step in the reaction and how the initial hydrogen shift effects or limits the subsequent reactions.

5. CONCLUSIONS

The present study has shown that upon excitation at wavelengths ranging from the S_0-S_1 origin (266.79 nm) to 193 nm benzylallene can undergo isomerization followed by H-atom/H_2 loss to form naphthalene in the gas phase. Subsequent preliminary studies of *trans*-1-phenyl-1,3-butadiene and 4-phenyl-1-butyne have provided convincing evidence that at lower excitation energies naphthalene is formed via an internal isomerization on the $C_{10}H_{10}$ surface leading to ring closure, followed by the loss of two hydrogen atoms (or H_2). A particular strength of the present study is its ability to selectively detect and characterize isomeric products through fast cooling followed by

wavelength- and mass-resolved detection via R2PI spectroscopy. To incorporate these results into current photochemical models of Titan's atmosphere, photochemical quantum yields for each product are needed.[4,5] It will also be important to determine with certainty whether ground state or excited state processes are of greater importance in naphthalene formation from benzylallene and 1-phenyl-1,3-butadiene. Under the conditions in Titan's atmosphere, UV photoexcitation of benzylallene is likely to produce naphthalene whether these processes occur in ground or excited states. If ground state processes dominate, the present results may also be of importance to naphthalene formation in a wider range of circumstances, most notably in combustion.

■ ASSOCIATED CONTENT

ⓈSupporting Information

Details of the synthesis and characterization of benzylallene and deuterated isotopomers; reactant and product timing diagrams for photochemical studies; and complete reference 18. This material is available free of charge via the Internet at http://pubs.acs.org.

■ AUTHOR INFORMATION

Corresponding Author
zwier@purdue.edu
Present Address
‖NASA Goddard Space Flight Center.

■ ACKNOWLEDGMENTS

■ REFERENCES

(1) Trainer, M. G.; Pavlov, A. A.; DeWitt, H. L.; Jimenez, J. L.; McKay, C. P.; Toon, O. B.; Tolbert, M. A. *Proc. Natl. Acad. Sci. U.S.A.* **2006**, *103*, 18035.

(2) Waite, J. H. Jr.; Young, D. T.; Cravens, T. E.; Coates, A. J.; Crary, F. J.; Magee, B.; Westlake, J. *Science* **2007**, *316*, 870.

(3) Coates, A. J.; Crary, F. J.; Lewis, G. R.; Young, D. T.; Waite, J. H.; Sittler, E. C. *Geophys. Res. Lett.* **2007**, *34*.

(4) Wilson, E. H.; Atreya, S. K. *J. Geophys. Res., [Planets]* **2004**, *109*, E06002.

(5) Krasnopolsky, V. A. *Icarus* **2009**, *201*, 226.

(6) Newby, J. J.; Stearns, J. A.; Liu, C. P.; Zwier, T. S. *J. Phys. Chem. A* **2007**, *111*, 10914.

(7) Stearns, J. A.; Zwier, T. S.; Kraka, E.; Cremer, D. *Phys. Chem. Chem. Phys.* **2006**, *8*, 5317.

(8) Miller, J. A.; Klippenstein, S. J. *J. Phys. Chem. A* **2001**, *105*, 7254.

(9) Miller, J. A.; Klippenstein, S. J. *J. Phys. Chem. A* **2003**, *107*, 7783.

(10) Selby, T. M.; Zwier, T. S. *J. Phys. Chem. A* **2005**, *109*, 8487.

(11) Pillsbury, N. R.; Zwier, T. S. *J. Phys. Chem. A* **2009**, *113*, 118.

(12) Pillsbury, N. R.; Zwier, T. S. *J. Phys. Chem. A* **2009**, *113*, 126.

(13) Sebree, J. A.; Kislov, V. V.; Mebel, A. M.; Zwier, T. S. *Faraday Discuss.* **2010**, *147*, 231.

(14) Sebree, J. A.; Kidwell, N. M.; Buchanan, E. G.; Zgierski, M. Z.; Zwier, T. S. *Chem. Sci.* **2011**, *2*, 1746.

(15) Landera, A.; Kaiser, R. I.; Mebel, A. M. *J. Chem. Phys.* **2011**, *134*, 024302.

(16) Becke, A. D. *Phys. Rev. A* **1988**, *38*, 3098.

(17) Lee, C.; Yang, W.; Parr, R. G. *PhRvB* **1988**, *37*, 785.

(18) Frisch, M. J., et al. *Gaussian 09*, Revision A.02; Gaussian, Inc.: Wallingford, CT, 2009.

(19) Plusquellic, D. F.; Suenram, R. D.; Mate, B.; Jensen, J. O.; Samuels, A. C. *J. Chem. Phys.* **2001**, *115*, 3057.

(20) Hopkins, J. B.; Powers, D. E.; Smalley, R. E. *J. Chem. Phys.* **1980**, *72*, 5039.

(21) Varsanyi, G. *Assignments for Vibrational Spectra of 700 Benzene Derivatives*; Wiley: New York, 1974.

(22) Dickinson, J. A.; Joireman, P. W.; Kroemer, R. T.; Robertson, E. G.; Simons, J. P. *J. Chem. Soc., Faraday Trans.* **1997**, *93*, 1467.

(23) Dickinson, J. A.; Joireman, P. W.; Randall, R. W.; Robertson, E. G.; Simons, J. P. *J. Phys. Chem. A* **1997**, *101*, 513.

(24) Pillsbury, N. R.; Choo, J.; Laane, J.; Drucker, S. *J. Phys. Chem. A* **2003**, *107*, 10648.

(25) Liu, C.-P.; Newby, J. J.; Muller, C. W.; Lee, H. D.; Zwier, T. S. *J. Phys. Chem. A* **2008**, *112*, 9454.

(26) Newby, J. J.; Liu, C.-P.; Muller, C. W.; James, W. H.; Buchanan, E. G.; Lee, H. D.; Zwier, T. S. *J. Phys. Chem. A* **2010**, *114*, 3190.

(27) Sebree, J. A.; Plusquellic, D. F.; Zwier, T. S. *J. Mol. Spectrosc.* **2011**, *270*, 98−107.

(28) Beck, S. M.; Powers, D. E.; Hopkins, J. B.; Smalley, R. E. *J. Chem. Phys.* **1980**, *73*, 2019.

(29) Buma, W. J.; Kohler, B. E.; Nuss, J. M.; Shaler, T. A.; Song, K. *J. Chem. Phys.* **1992**, *96*, 4860.

(30) Chakraborty, T.; Chowdhury, M. *Spectrochim. Acta, Part A* **1992**, *48*, 1683.

(31) Alabugin, I. V.; Manoharan, M.; Breiner, B.; Lewis, F. D. *J. Am. Chem. Soc.* **2003**, *125* (31), 9329−9342.

(32) Badger, G. M.; Spotswood, T. M. *J. Chem. Soc. (Resumed)* **1959**, 1635.